H1prelim-08-034 Submitted to

XVI International Workshop on Deep-Inelastic Scattering, DIS2008, April 7-11, 2008, London
Parallel Session **Hadronic Final State and QCD**

Electronic Access:https://www-h1.desy.de/publications/H1preliminary.short_list.html

Strangeness Production in Deep-inelastic ep Scattering at HERA

H1 Collaboration

Abstract

The production of the neutral strange mesons K_s^0 and the strange baryons Λ and their antiparticles is investigated using deep inelastic scattering events measured with the H1 detector at HERA. The K_s^0 and Λ production cross sections and the baryon to meson ratios are reported differentially for the range of negative photon four-momentum transfer squared $2 < Q^2 < 100\ \mathrm{GeV}^2$ and photon inelasticity $0.1 < y < 0.6$. In addition, the K_s^0 production rates are compared directly with those of charged particles in the same phase space region. The $\Lambda - \bar{\Lambda}$ asymmetry is also measured differentially and found to be consistent with zero in all bins.

The model predictions, based on leading order Monte Carlo programs in general are able to describe the overall features of the measurements, however fail in particular details. The data agree with the expectations from e^+e^- colliders.

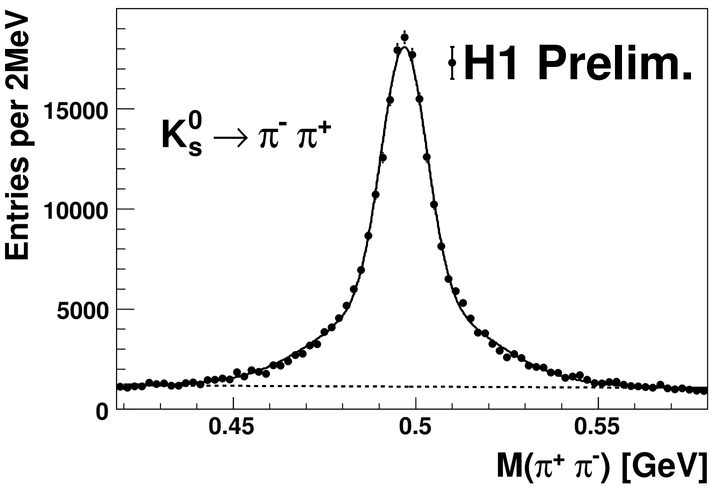

Figure 1: The invariant mass spectra for $\pi^+\pi^-$ particle combinations. The solid lines show the result of a fit to the data using two Gaussian functions for the K_s^0 signal and a background function while the dashed lines indicate the background function only. The data are shown as black points with error bars denoting total uncertainty.

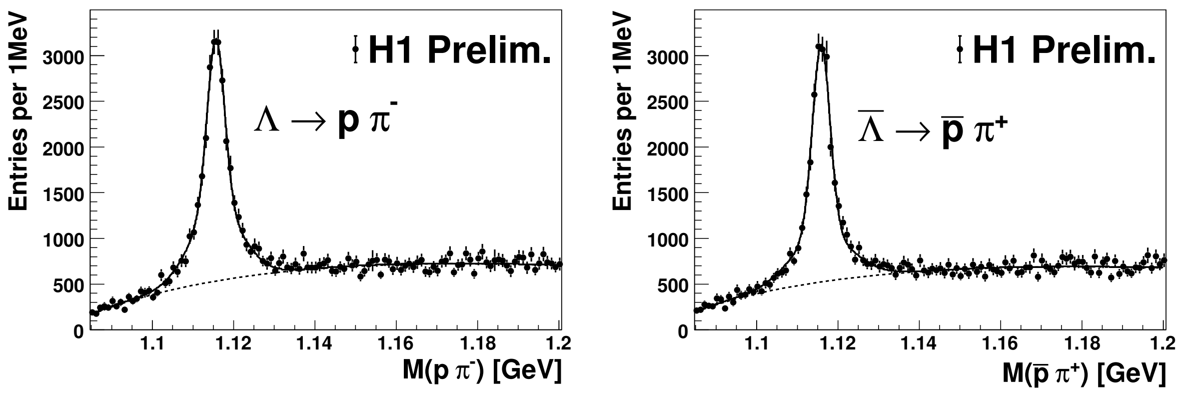

Figure 2: The invariant mass spectra for a) $\Lambda \to p\pi^-$ and b) $\bar{\Lambda} \to \bar{p}\pi^+$ particle combinations. The solid lines show the result of a fit to the data using two Gaussian functions for the Λ and the Λ signal, and the background function while the dashed lines indicate the background function only. The data are shown as black points with error bars denoting total uncertainty.

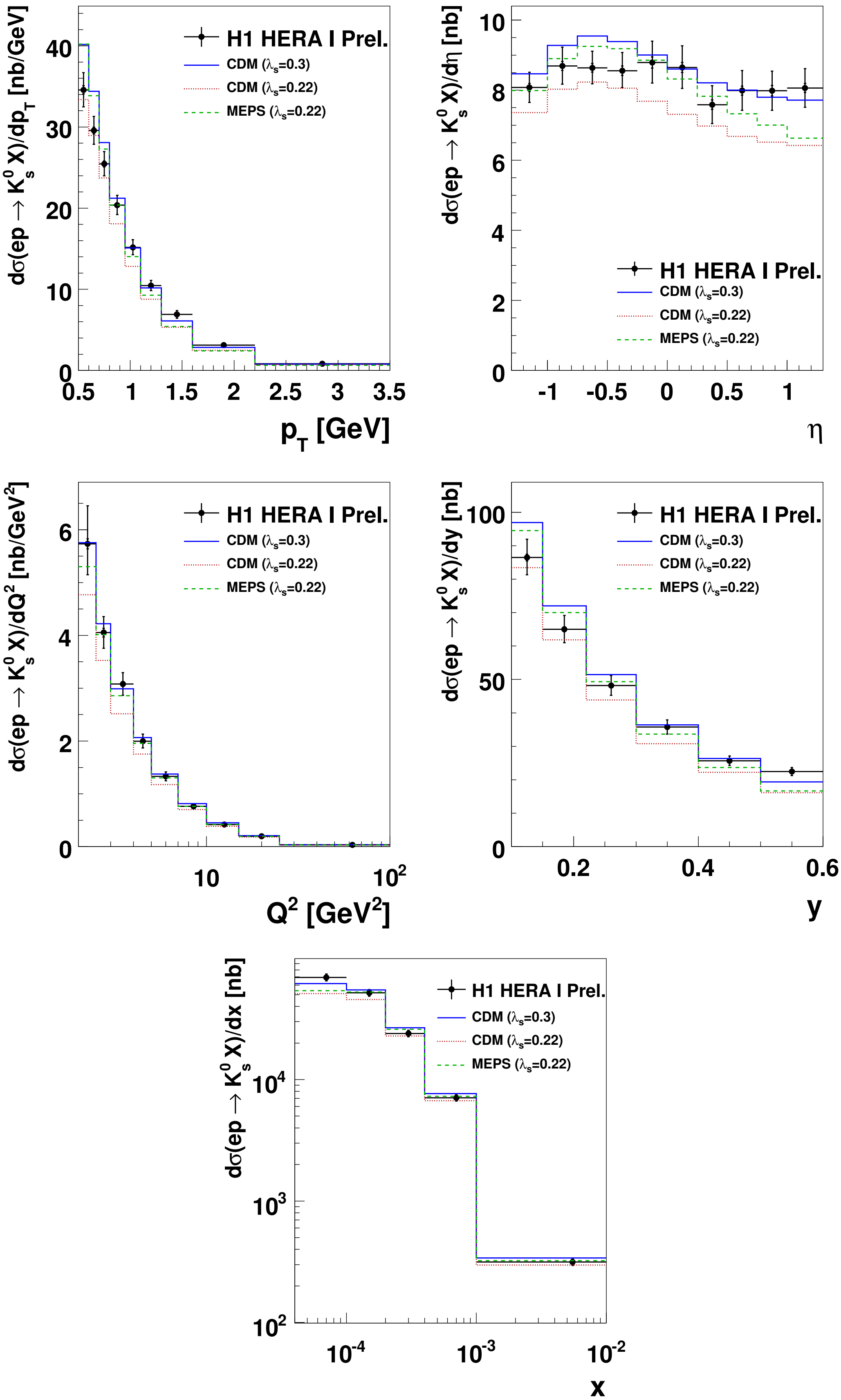

Figure 3: The differential production cross sections for K_s^0 in the laboratory frame as a function of the K_s^0 transverse momentum p_{T} and the K_s^0 pseudorapidity η in the laboratory frame and of the event variables: photon virtuality squared Q^2 , photon inelasticity y and Bjorken scaling variable x. The error bars show full uncertainty. The lines show the different LO Monte Carlo predictions .

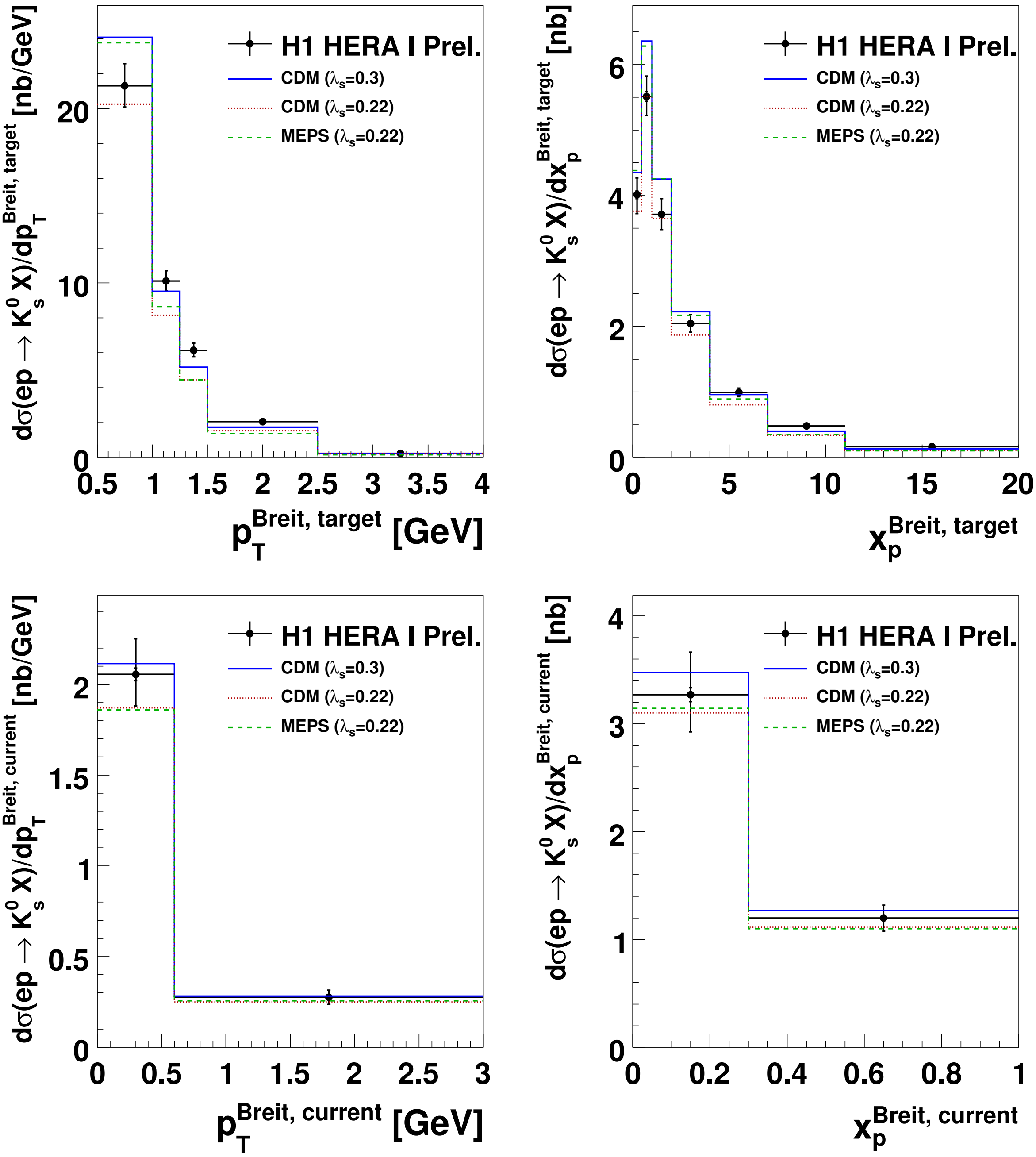

Figure 4: The differential K_s^0 production cross sections measured in the Breit frame as a function of the K_s^0 transverse momentum p_T and the momentum fraction $x_{P,breit}$ both in the current and in the target frame.

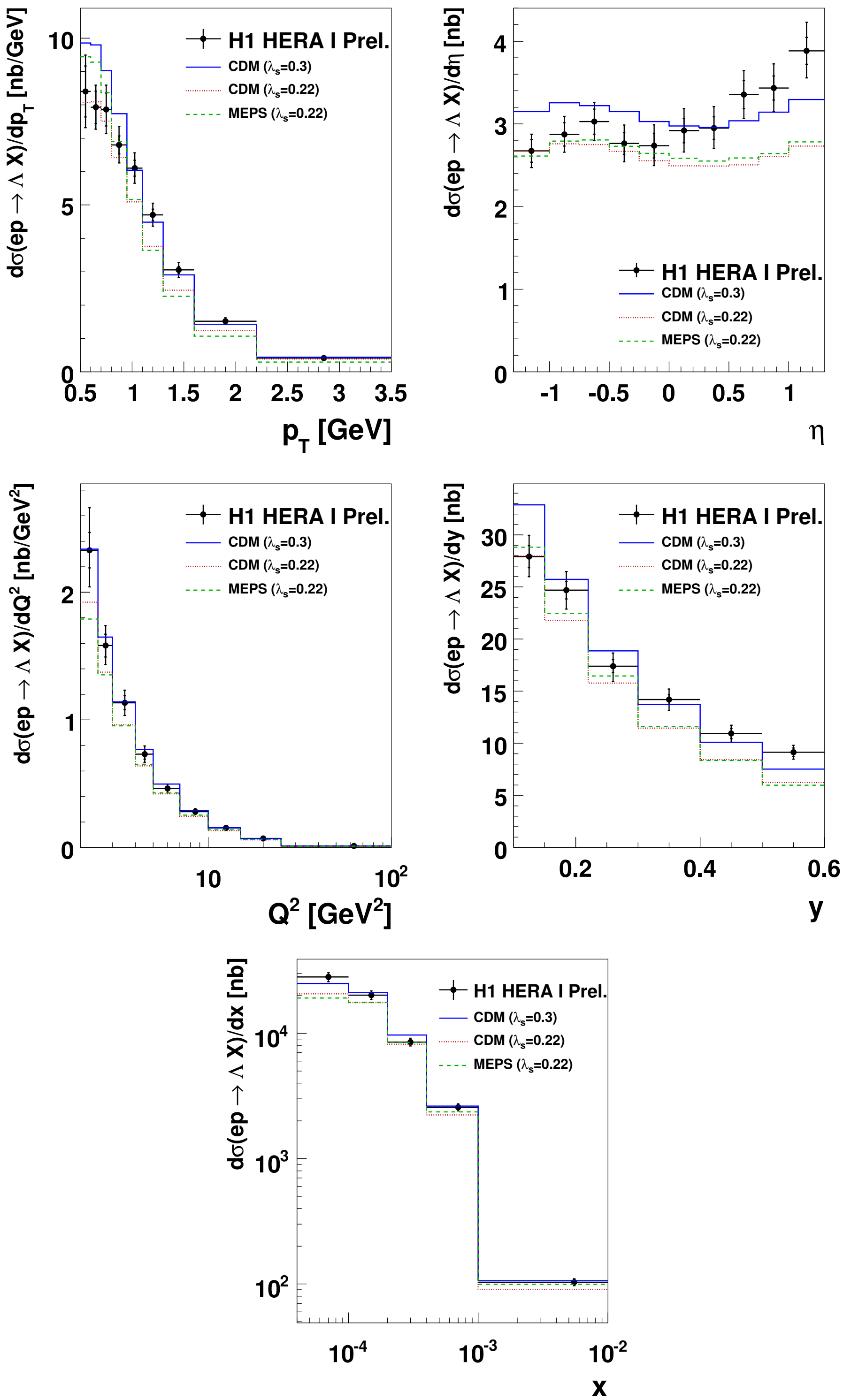

Figure 5: The differential production cross sections for Λ in the laboratory frame as a function of the Λ transverse momentum p_T and the Λ pseudorapidity η, and of the event variables: photon virtuality squared Q^2 , photon inelasticity y and Bjorken scaling variable x. The error bars show the statistical (inner bars) and the total (outer bars) errors, respectively. The lines show the predictions of the LO Monte Carlo programs. .

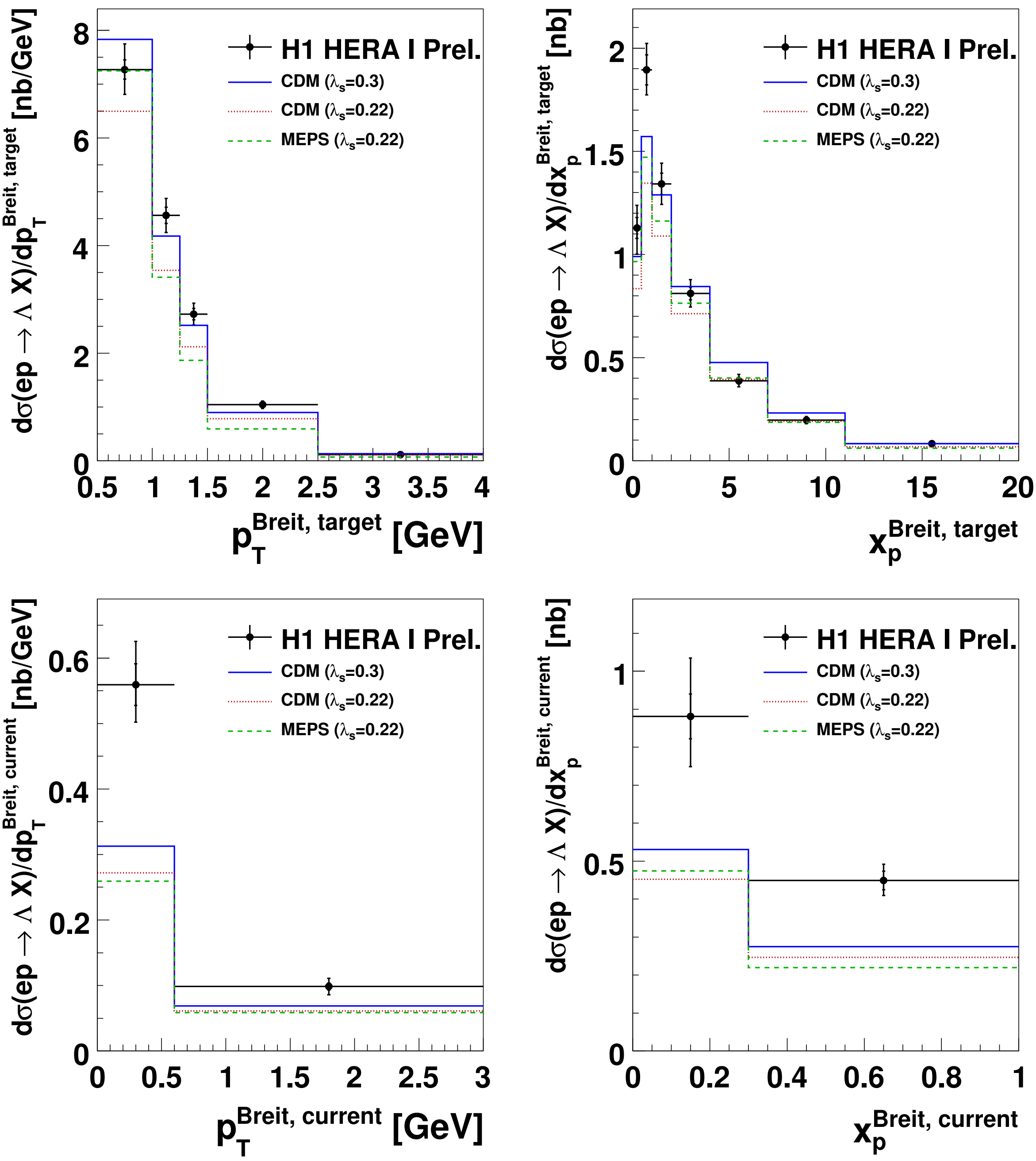

Figure 6: The differential production cross sections for the sum of Λ and $\bar{\Lambda}$ baryons measured in the Breit frame as a function of the Λ transverse momentum p_T and the momentum fraction $x_{P,breit}$ both in the current and in the target frame.

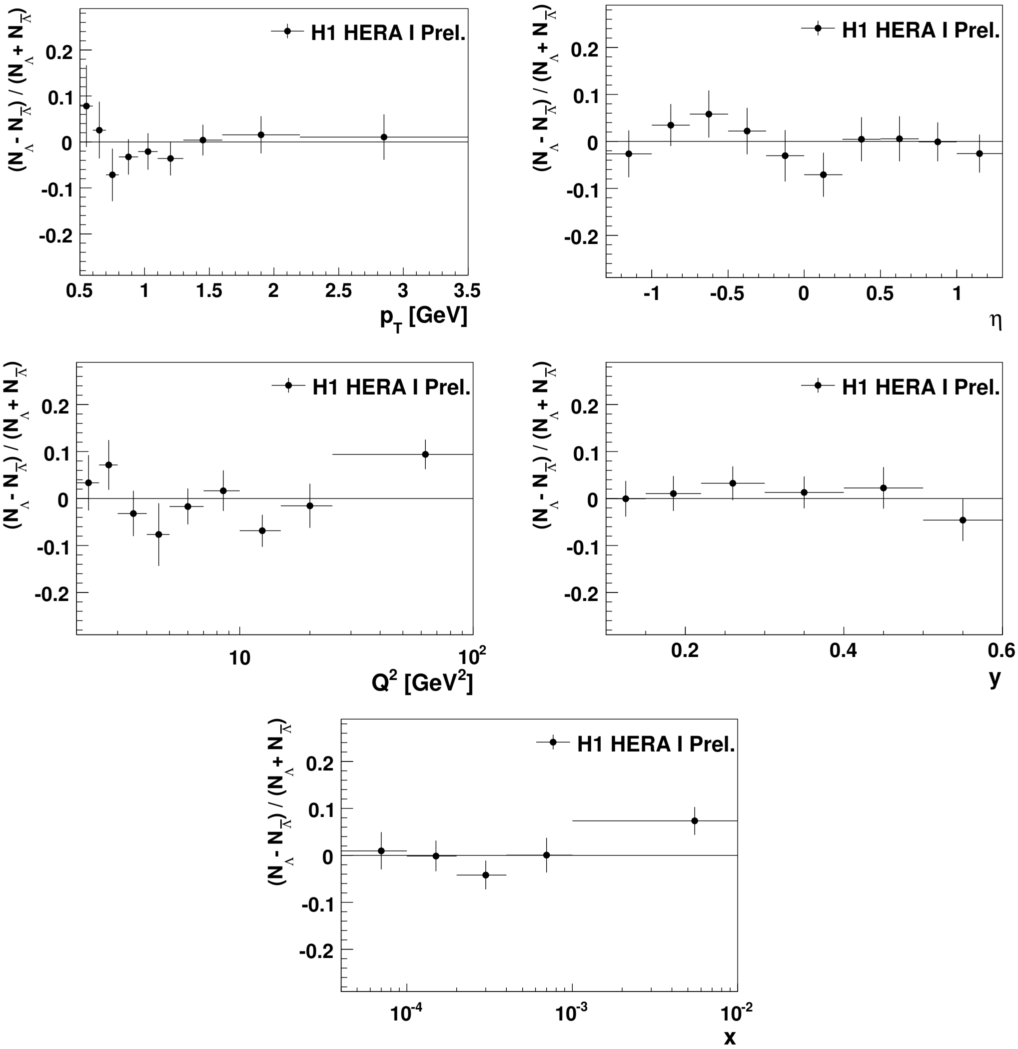

Figure 7: The differential production cross sections for the Λ to $\bar{\Lambda}$ baryon asymmetry in the laboratory frame as a function of the Λ transverse momentum p_{T} and the pseudorapidity η, and of the event variables: photon virtuality squared Q^2 , photon inelasticity y and Bjorken scaling variable x. The error bars show the statistical uncertainty. The solid lines show the predictions of the LO Monte Carlo program CDM .

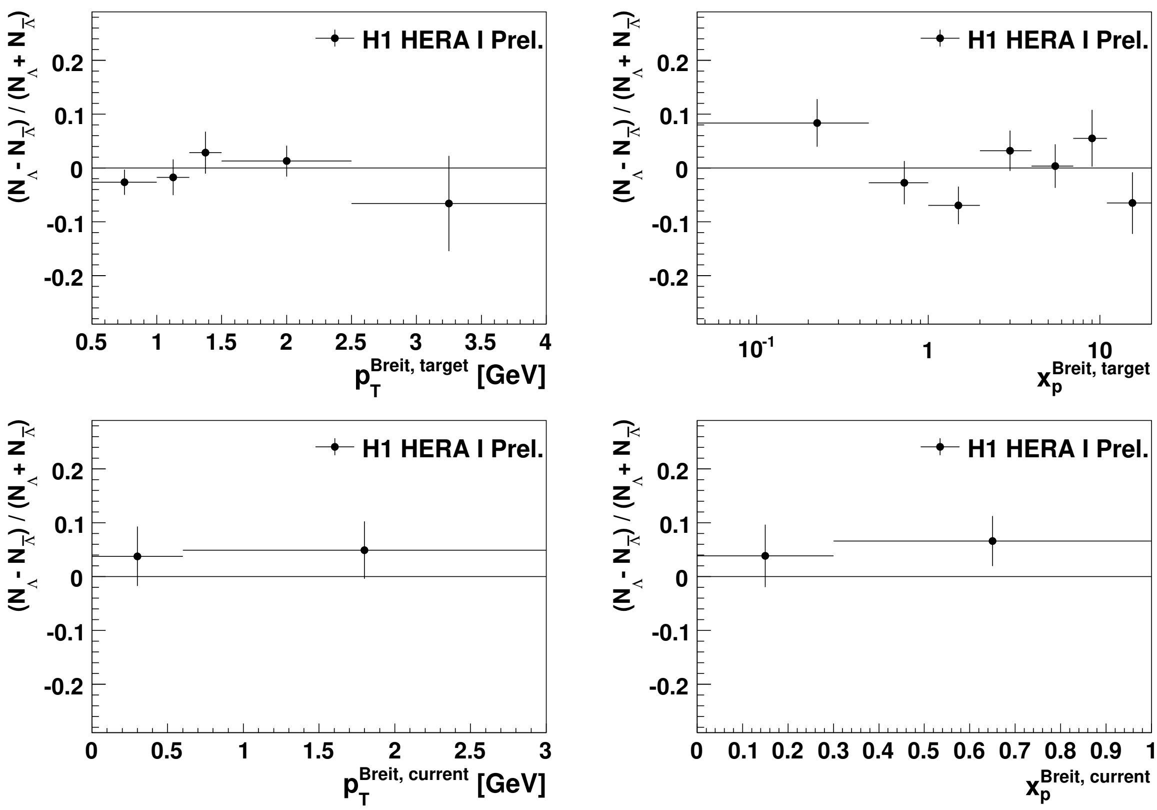

Figure 8: The differential production cross sections for the Λ to $\bar{\Lambda}$ baryon asymmetry measured in the Breit frame as a function of the Λ transverse momentum p_T and the momentum fraction $x_{P,breit}$ both in the current and in the target frame.

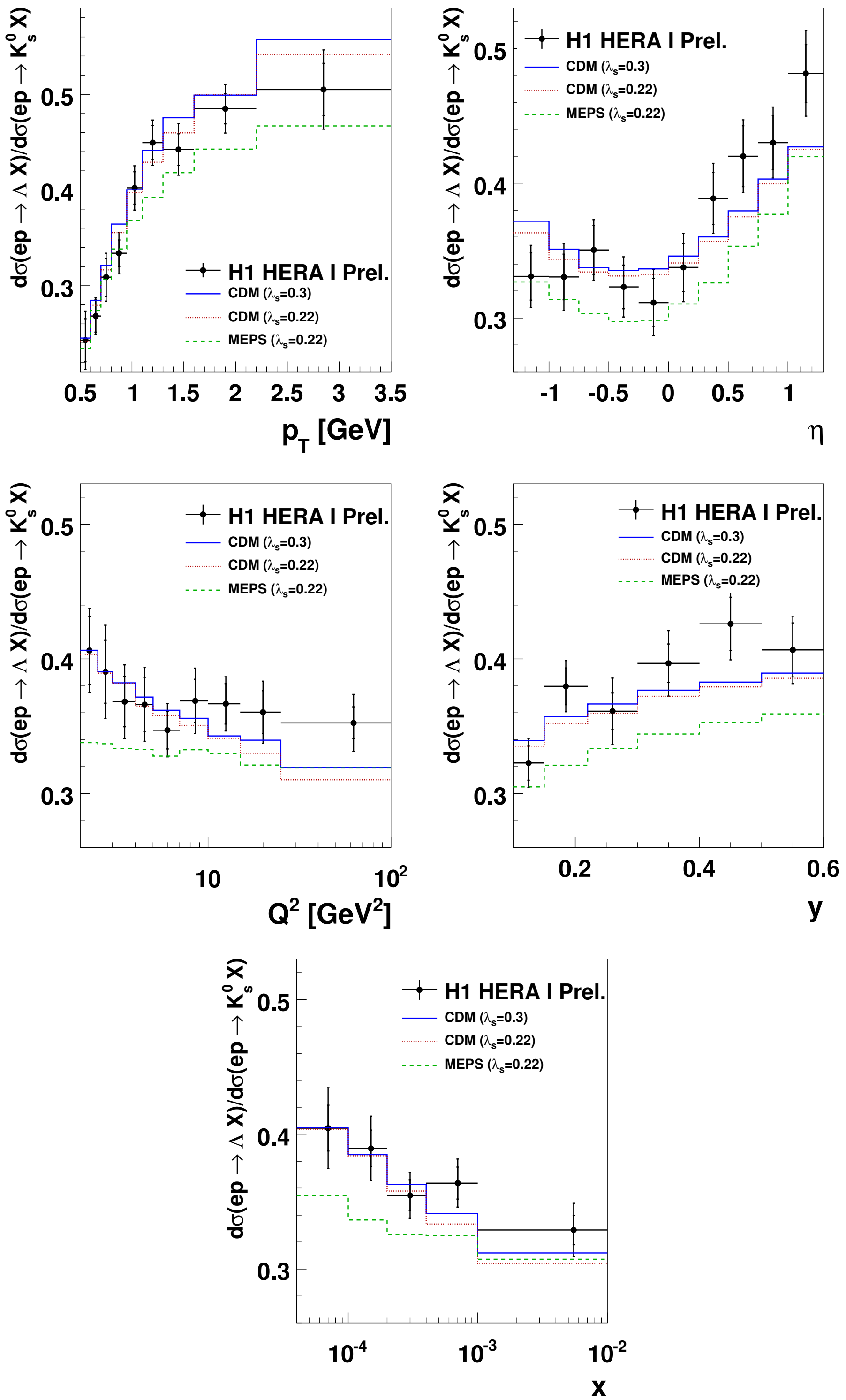

Figure 9: The differential production cross sections for the Λ baryon to K_s^0 meson ratio in the laboratory frame as a function of the transverse momentum p_{T} and the pseudorapidity η, and of the event variables: photon virtuality squared Q^2 , photon inelasticity y and Bjorken scaling variable x. The error bars show the statistical uncertainty. The lines show the predictions of the LO Monte Carlo programs .

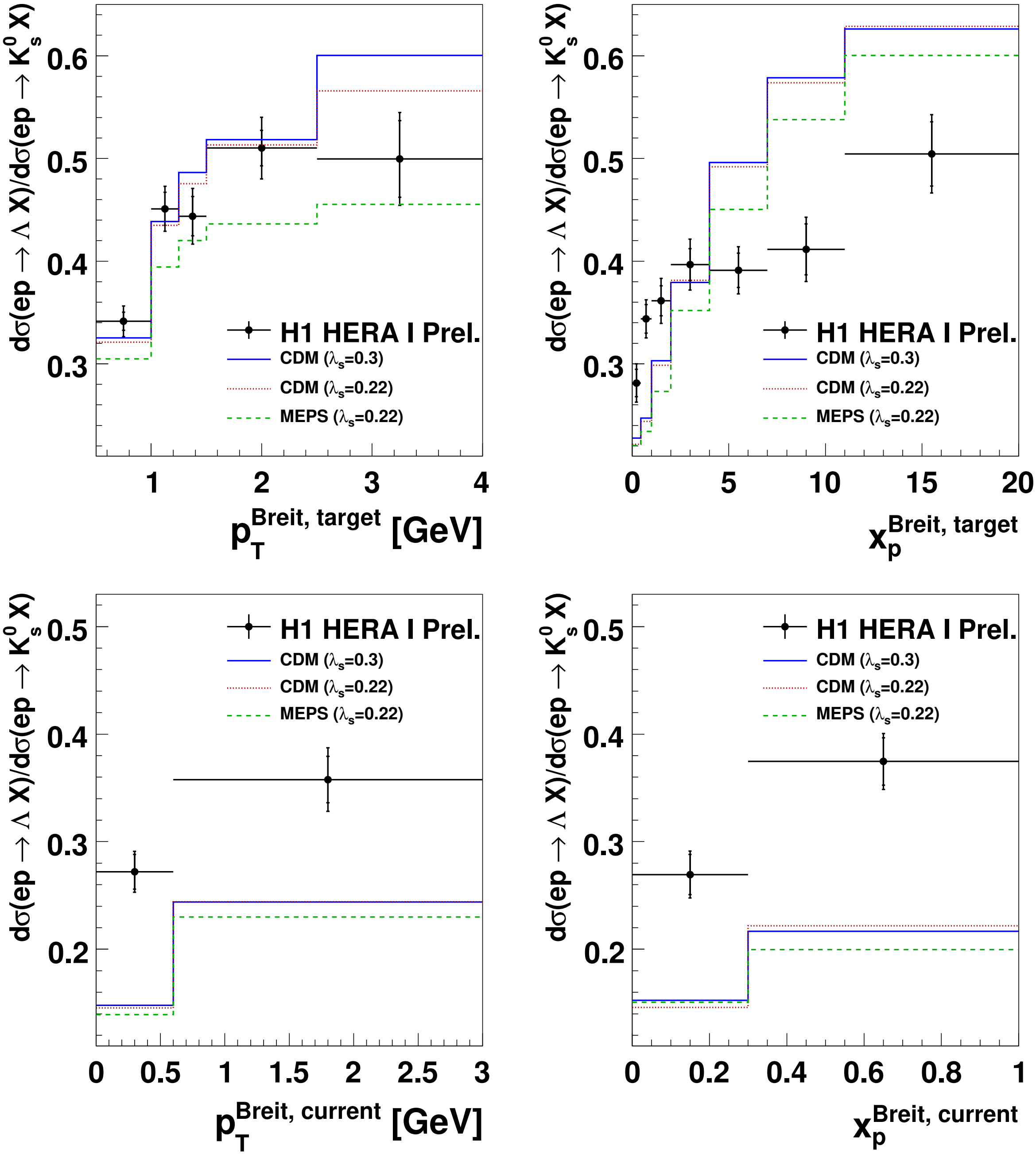

Figure 10: The differential production cross sections for the Λ baryon to K_s^0 meson ratio measured in the Breit frame as a function of the transverse momentum p_T and the momentum fraction $x_{P,breit}$ both in the current and in the target frame.

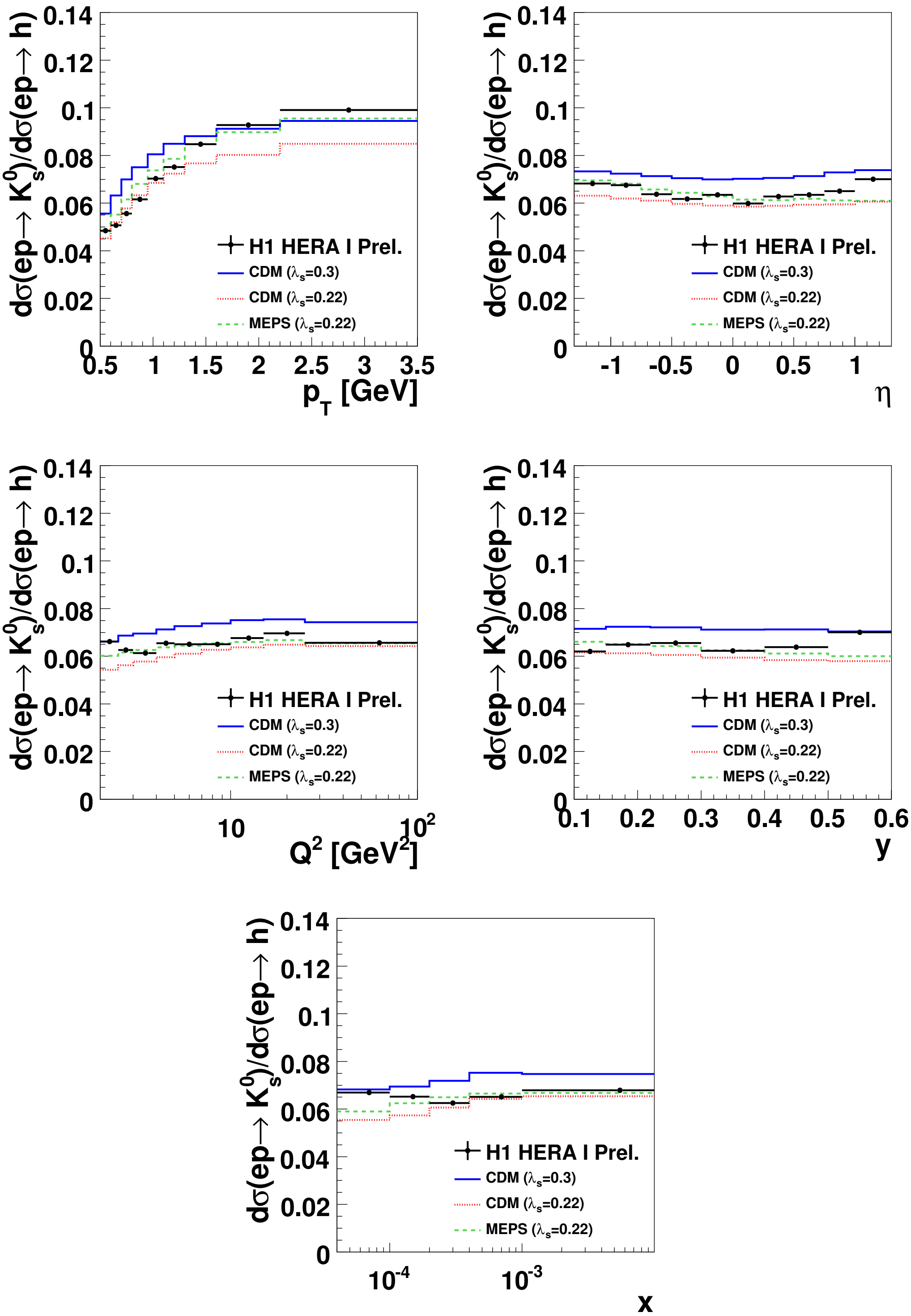

Figure 11: The differential production cross sections for the K_s^0 meson to charged hadrons ratio in the laboratory frame as a function of the transverse momentum p_T and the pseudorapidity η, and of the event variables: photon virtuality squared Q^2 , photon inelasticity y and Bjorken scaling variable x. The error bars show the total uncertainty. The lines show the predictions of the LO Monte Carlo programs. .

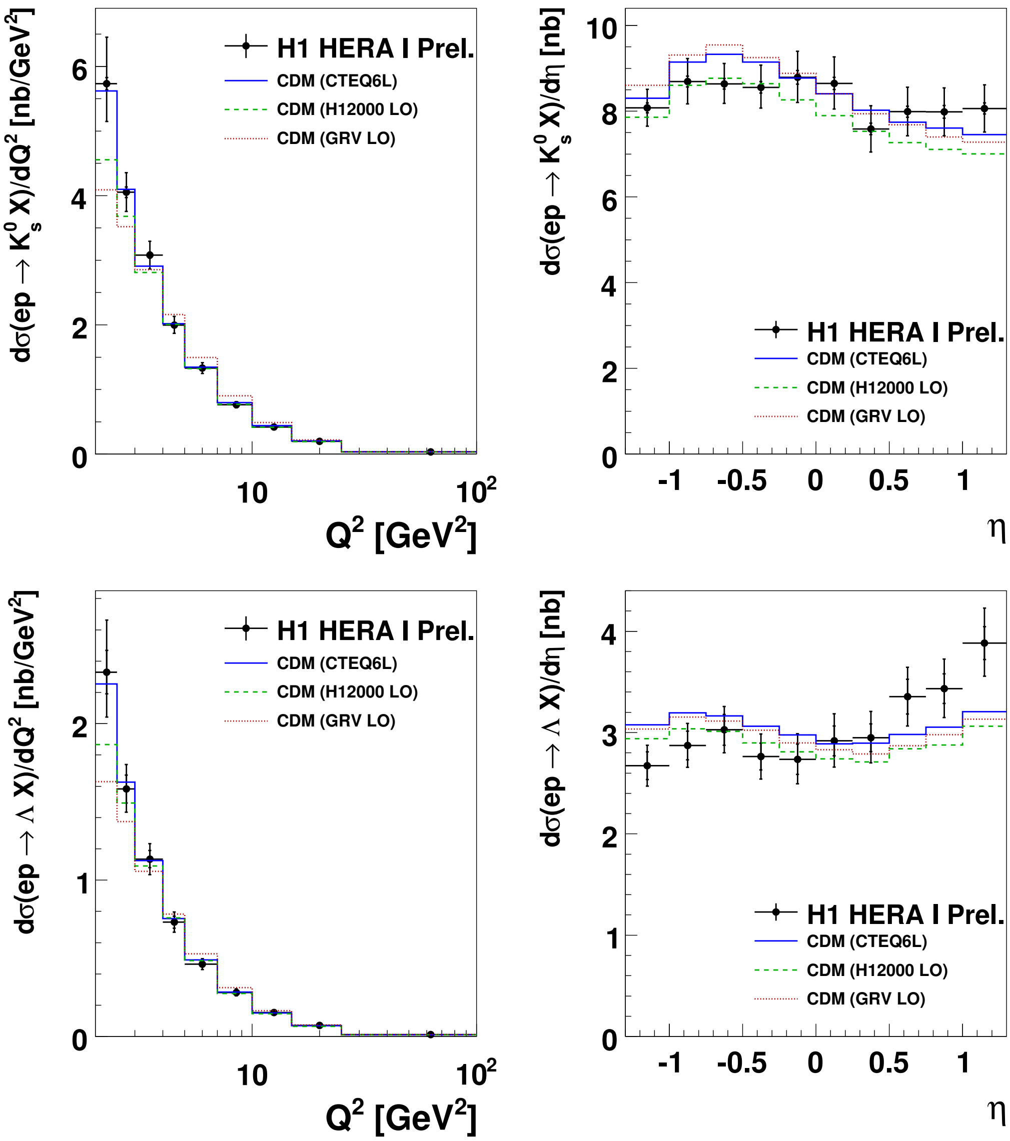

Figure 12: The differential production cross sections for K_s^0 and Λ in the laboratory frame as a function of the event variable Q^2 and the pseudorapidity η. Overlaid are predictions by various proton PDFs: CTEQ6L, GRV LO, H12000 LO.